



ELSEVIER

Termination of equine atrial fibrillation by quinidine: An optical mapping study[☆]

Flavio H. Fenton, PhD^a, Elizabeth M. Cherry, PhD^a,
Bruce G. Kornreich, DVM, PhD^{b,*}

^a *Department of Biomedical Sciences, Cornell University, Ithaca, NY 14853, USA*

^b *Department of Clinical Sciences, Cornell University, Ithaca, NY 14853, USA*

Received 31 July 2008; received in revised form 30 September 2008; accepted 8 October 2008

KEYWORDS

Atrial fibrillation;
Alternans;
Quinidine;
Restitution;
Optical mapping

Abstract *Objective:* To perform the first optical mapping studies of equine atrium to assess the spatiotemporal dynamics of atrial fibrillation (AF) and of its termination by quinidine.

Animals: Intact, perfused atrial preparations obtained from four horses with normal cardiovascular examinations.

Materials and methods: AF was induced by a rapid pacing protocol with or without acetylcholine perfusion, and optical mapping was used to determine spatial dominant frequency distributions, electrical activity maps, and single-pixel optical signals. Following induction of AF, quinidine gluconate was perfused into the preparation and these parameters were monitored during quinidine-induced termination of AF.

Results: Equine AF develops in the context of spatial gradients in action potential duration (APD) and diastolic interval (DI) that produce alternans, conduction block, and Wenckebach conduction in different regions at fast pacing rates. Quinidine terminates AF and prevents subsequent reinduction by reducing the maximal frequency and increasing frequency homogeneity.

Conclusions: Heterogeneity of APD and DI promote alternans and conduction block at fast pacing rates in the equine atrium, predisposing to the development of AF.

[☆] A unique aspect of the Journal of Veterinary Cardiology is the emphasis of additional web-based images permitting the detailing of procedures and diagnostics. These images can be viewed (by those readers with subscription access) by going to <http://www.sciencedirect.com/science/journal/17602734>. The issue to be viewed is clicked and the available PDF and image downloading is available via the Summary Plus link. The supplementary material for a given article appears at the end of the page. Downloading the videos may take several minutes. Readers will require at least Quicktime 7 (available free at <http://www.apple.com/quicktime/download/>) to enjoy the content. Another means to view the material is to go to <http://www.doi.org> and enter the doi number unique to this paper which is indicated at the end of the manuscript.

* Corresponding author.

E-mail address: bgk2@cornell.edu (B.G. Kornreich).

Quinidine terminates AF by reducing maximum frequency and increasing frequency homogeneity. Our results are consistent with the hypothesis that quinidine increases effective refractory period, thereby decreasing frequency.

© 2008 Elsevier B.V. All rights reserved.

Introduction

Atrial fibrillation (AF) is the most commonly diagnosed cardiac arrhythmia in horses, with prevalence ranging as high as 2.5% depending upon study population.^{1–4} Although AF is commonly diagnosed as an incidental finding in horses, it remains a significant cause of poor performance in equine athletes, and as such constitutes an important disease entity in equine patients.^{5–7} Horses are presumably predisposed to AF primarily due to their high vagal tone and large atrial mass,^{4,8–11} which combine to promote the maintenance of multiple reentrant circuits, or spiral waves, within the atria of affected individuals. While the spatiotemporal behavior of these spiral waves has been the subject of considerable research and debate, it is generally accepted that they are responsible for the rapid, apparently irregular atrial depolarizations that are characteristic of AF.^{10–18}

The ideal treatment of human patients with AF is conversion to normal sinus rhythm (NSR), as chronic AF is associated with increased risk of thromboembolism, stroke, and cardiovascular death in people.^{19–22} While these associations have not been documented in equine patients, AF is a well documented cause of poor performance in the horse.^{22–24} For this reason, although long-standing AF or significant structural heart disease may preclude successful conversion, many equine patients with AF of relatively short duration (i.e., less than four months) and no significant structural cardiac pathology (termed lone AF) are converted to NSR using either pharmacologic or electrical modalities.^{23,24} The requirement for anesthesia, specialized equipment, and expertise for electrical cardioversion, however, combined with the relatively high success rate of pharmacologic cardioversion, precludes electrical cardioversion in most equine patients. Given these considerations, the vast majority of equine AF patients are converted pharmacologically using orally administered drugs.

Quinidine is the most commonly used drug to convert equine patients with AF to NSR.^{7,28} This Class IA antiarrhythmic drug decreases the maximum rate of rise of phase 0 depolarization via

sodium channel blockade and prolongs repolarization via blockade of a number of potassium channels (most notably I_{kr}) in myocardial tissue.^{29–37} The net effects of these actions are to decrease conduction velocity and to prolong action potential duration and effective refractory period in atrial, ventricular, and Purkinje myocytes.^{37–42} These actions are believed to form the basis for their effectiveness in interrupting reentrant circuits that underlie AF, and a number of studies have shown that quinidine is efficacious at converting the majority of equine fibrillation patients with lone AF to NSR.^{7,28,43,44}

In spite of its relatively high clinical efficacy at converting horses in AF to NSR, the definitive spatiotemporal mechanism by which quinidine achieves this conversion in horses remains unclear. Given the prevalence and clinical impact of equine AF, the frequency at which quinidine is administered to equine patients with AF, and the potential role that horses may play as a viable animal model of human AF, an understanding of the mechanism by which quinidine terminates AF in horses is likely to provide information that not only will be useful to clinical veterinarians, but also will improve our understanding of AF in other species, including humans.

Optical mapping using voltage-sensitive dyes has been used previously to investigate both mechanisms of arrhythmogenesis and of pharmacologic and electrical termination of arrhythmias.^{45–53} This technique has proven valuable in the study of both atrial and ventricular arrhythmias and has been applied to a wide variety of species including human, dog, sheep, swine, rabbit, guinea pig, mouse, and rat.^{46,54–64} Optical mapping has not been applied to the study of atrial fibrillation in horses, to our knowledge.

We designed a series of optical mapping experiments using intact equine atrial preparations perfused with the voltage-sensitive dye di-4-ANEPPS^{16,65–69} to test the hypotheses that quinidine terminates AF, and that this termination is associated with a measurable change in AF dominant frequency. To our knowledge, this is the first application of optical mapping to study the mechanism of an antiarrhythmic drug in isolated equine cardiac preparations.

Animals, materials and methods

Tissue harvesting and perfusion

All experiments were carried out in accordance with IACUC guidelines in AAALAC-approved facilities. Immediately following euthanasia of horses of either gender for non-cardiac reasons ranging from career-ending musculoskeletal abnormalities to blindness, hearts were removed (Fig. 1A) and placed in 22–25 °C Tyrode solution containing (in mM): MgCl₂ 2, NaH₂PO₄ 0.9, CaCl₂ 2, NaCl 137, NaHCO₃ 24, KCl 4, Glucose 5.5.⁷⁰ All Tyrode solution was equilibrated with 95% oxygen/5% CO₂. The atria were then dissected from the heart (Fig. 1B) and the coronary vasculature was cannulated with flexible tubing (1/4 inch ID, 1/16 inch wall thickness; Fisher Scientific Co, Pittsburgh, PA) that was sutured into the coronary ostium immediately distal to the aortic valve leaflets using silk suture material in a simple continuous suture pattern (Ethicon Inc., Piscataway, NJ). Perfusion of the excised atrium via the coronary vasculature with 37 °C Tyrode solution was instituted at a rate of 40 ml/min. This flow rate was extrapolated from rates established for canine cardiac preparations, accounting for increased tissue mass. Viability of the preparation was assessed by visual inspection for normal contraction at a rate of approximately 30 beats per minute (see [Supplemental movie](#)). Leakage from the cut edges of the preparation was prevented by suturing using silk suture material in a simple continuous pattern.

Optical mapping

The preparations were placed in a plexiglas chamber that kept the tissue submerged in Tyrode

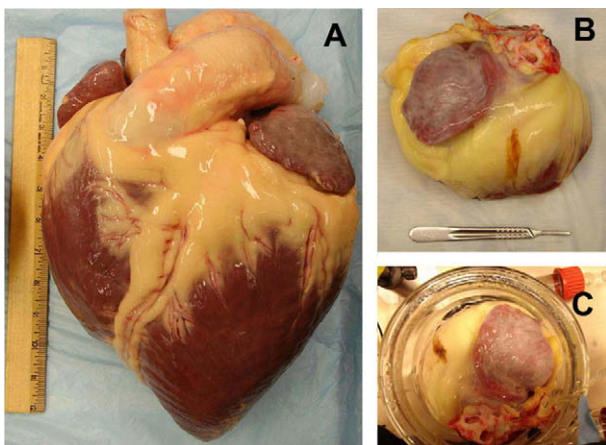


Figure 1 Equine heart and optical mapping setup. (A) Equine heart. (B) Equine left atrium. (C) Equine left atrial preparation in optical mapping setup.

and at 37 °C, as shown in Fig. 1C. To stain the tissue for optical mapping, the tissue was perfused with a single administration of 2 μM di-4-ANEPPS (Invitrogen Corporation, Carlsbad, CA) in 200 ml Tyrode solution; if necessary, staining was repeated halfway through the experiment. Preparations were perfused with Tyrode solution (with or without ACh or quinidine as required) and no perfusate was recirculated. Illumination was provided by nine high-power LEDs (Luxeon III star, LXHL-FM3C) at an excitation frequency of 530 ± 20 nanometers (nm). Fluorescence emission light was collected by a Navitar lens (DO-2595, focal length 25 mm, F/# 0.95, distance 60 cm), passed through a long-pass filter (<610 nm), and imaged by a 128 × 128 back-illuminated EMCCD array (electron-multiplied charge coupled device, Photometrics Cascade 128+). This camera provides high quantum efficiency (peak QE > 90%). The signal was digitized with a 16-bit A/D converter at frame rates of 511 Hz (full frame, 128 × 128 pixels). The PCI interface provides high-bandwidth uninterrupted data transfer to the host computer. Optical recordings were performed in episodes lasting 16–20 s and were obtained continuously during quinidine administration.

To prevent contraction and resultant motion artifact, 10–15 μM of blebbistatin, a myosin II inhibitor (BIOMOL International, Plymouth Meeting, PA), was added to Tyrode solution and perfused into the preparation for approximately 60 min prior to data collection. This concentration of blebbistatin has been used previously to prevent contraction of cardiac preparations in our laboratory and in other studies and has been shown to exert minimal effects on the electrophysiological properties of cardiac tissue.⁷¹ Microelectrode recordings (Fig. 2) show that blebbistatin has minimal effects on equine ventricular action potential amplitude, morphology, and duration and for a broad range of CLs.

Microelectrode recordings

Microelectrode recordings were performed on thin slices of ventricular tissue from the epicardium mounted in a Plexiglas chamber and superfused with normal Tyrode solution at a rate of 15 ml/min. The tissue was then stimulated using rectangular pulses of 2 ms duration and two to three times the diastolic threshold (0.1–0.3 mA) delivered through Teflon-coated bipolar silver electrodes using a computer-controlled stimulator. Transmembrane action potentials were recorded from the epicardium with machine-pulled glass capillary electrodes filled with 3 M KCl. Recordings

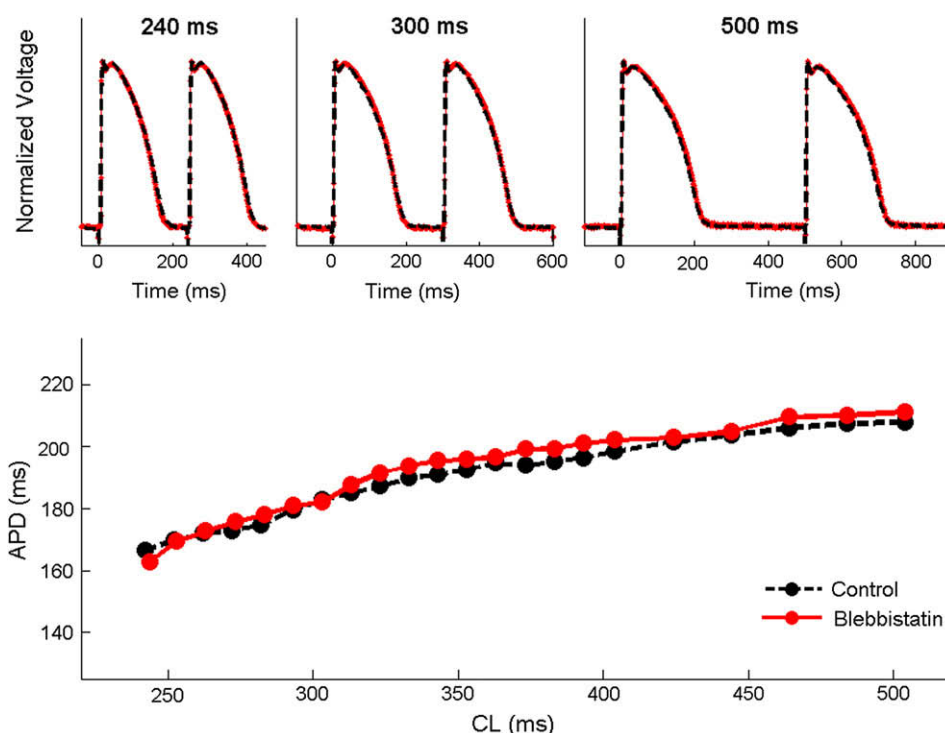


Figure 2 Use of blebbistatin to suppress contraction. With the application of blebbistatin, contraction and the resulting motion that can distort optical mapping signals can be avoided without affecting action potential and rate adaptation properties. Top: action potentials obtained from microelectrode recordings in equine ventricular tissue (epicardial) from three cycle lengths (240, 300, and 500 ms) before (black) and after (red) administration of 10–15 μM blebbistatin are nearly indistinguishable. Bottom: Rate adaptation curves obtained over a range of cycle lengths before (black) and after (red) blebbistatin administration in equine ventricular tissue (epicardial) show excellent agreement. Action potential durations (APDs) are computed as 90 percent of repolarization.

were obtained from sites located within 3–4 mm of the bipolar stimulating electrode. Restitution curves were obtained using protocols as described by Cherry and Fenton.⁷²

Initiation of fibrillation

The intact atrial preparation was paced at a cycle length (CL) of 500 ms using a bipolar stimulating electrode connected to an external pulse generator (Isostim A320, WPI Inc, Sarasota, Fla) delivering between 0.3 and 0.9 mA of current at a pulse duration of 3 ms until consistent capture was verified. For all experiments, the pacing electrode was placed on the epicardium of the free wall of the atrium, anatomically distant from the junction with the pulmonary veins, and the region mapped was along a line with end points at the pacing electrode and the opposite border of the atrium, defined as the border farthest from the pacing site. Fibrillation was initiated by a rapid pacing protocol beginning with a CL of 250 ms and decreasing by increments of 50 ms until fibrillation was initiated, as assessed by real-time monitoring of single pixels (similar to atrial electrograms) for the onset of

rapid, irregular signals. If rapid pacing alone did not initiate fibrillation, 1 μM acetylcholine (ACh) (acetylcholine chloride, Sigma–Aldrich, Milwaukee, WI) was added to the Tyrode perfusate and the pacing protocol reinstated until sustained fibrillation was initiated. If 1 μM ACh did not initiate fibrillation, serial increases in ACh concentration were carried out (in μM : 2, 4, 6, 8, 10, 20) until fibrillation was initiated and sustained.

Non-inducible, non-sustained, and sustained AF

Sustained AF was defined as fibrillation that lasted longer than 3 min. Non-inducible AF was defined as fibrillation that lasted three seconds or less. Atrial fibrillation that lasted between 3 s and 3 min was defined as non-sustained.

Quinidine use and AF termination or prevention

Once fibrillation was initiated, the preparation was perfused with quinidine gluconate (Eli Lilly and Co., Indianapolis, IN) in Tyrode solution beginning

with a concentration of $1.2\ \mu\text{M}$ and progressing through 6, 12, and $24\ \mu\text{M}$ concentrations until fibrillation was terminated or 10 min of perfusion with a given quinidine concentration had elapsed. These concentrations were chosen to determine dose response based upon previously documented serum quinidine levels in horses given intravenous quinidine gluconate at clinically relevant doses ($2\text{--}5\ \text{mg/ml}$), correcting for 20% protein binding of quinidine that has been established in horse serum.^{28,73} A minimum of 4 rapid pacing protocols was applied to a particular preparation at a given quinidine concentration before characterizing that concentration as preventive of AF. A trial was defined as either the initial pacing protocol applied to each preparation or to that applied after a change in ACh or quinidine concentration.

Data analysis

The dominant frequency of single pixels was calculated in real time during the experiments. Offline, optical action potentials were determined at every pixel by inverting the recorded fluorescence signal (as the fluorescence is inversely proportional to the membrane potential). Signal drift for each pixel was removed by subtracting the line connecting successive resting membrane potentials immediately preceding action potential upstrokes unless minima were not easily detectable (during some episodes of AF), in which case a low-pass filter was used instead. For each pixel, action potentials were then normalized to the signal maximum and minimum of the time series to obtain a normalized voltage (NV) signal. Signals were subsequently averaged in time with a nearest-neighbor method and in space using a Gaussian function with a 3-pixel radius to reduce noise.

Action potential durations (APD) were measured to 90 percent repolarization. Isochrones were calculated from the activation times computed at each pixel by determining when an action potential upstroke reached 50 percent of the action potential amplitude and by using a spatial filter consisting of a weighted average of nearest neighbors to smooth outlying points. Spatial frequency maps were determined by computing the power spectrum of each pixel within a 1–8 s window and selecting the maximum frequency as the dominant frequency. We verified that the frequency maps did not change significantly by choosing longer or shorter windows when the arrhythmia was stable, and we chose shorter window lengths to illustrate changes in arrhythmia characteristics during termination.

Results

Conduction in normal atria

Six equine atrial preparations were studied, with four achieving adequate perfusion and staining with di-4-ANEPPS to provide sufficient signal-to-noise ratio for data collection. Representative optical action potentials obtained during pacing to steady state at different cycle lengths (CLs) are shown in Fig. 3. Action potential durations measured at 90 percent of repolarization were obtained at four sites in a single preparation over a range of CLs and are plotted in Fig. 3 as a function of CL (rate adaptation curve) and of diastolic interval (DI) (restitution curve). These curves show two important properties. First, the restitution curve is steep, with slope greater than one (slope >1 for DIs $<70\ \text{ms}$, maximum slope of 3.2), indicating a large decrease in action potential duration with small decreases in CL at rapid pacing rates. Despite the steepness of the restitution curve, no alternans were present close to the pacing site. Second, the minimum CL or DI for which action potentials could be obtained varied among the sites and constitute spatial heterogeneity in the tissue. Because of this variation, at short CLs part of the tissue with a higher minimum DI cannot support 1:1 propagation, resulting in 2:1 conduction block in which only every other beat propagates. This effect is further demonstrated in Fig. 4, where isochrones are shown for a long CL of 750 ms and for a short CL of 250 ms. At the long CL (Fig. 4A), although regions of conduction slowing can be observed, the entire tissue responds to every paced beat in a 1:1 manner. At the short CL, however, the pacing cannot capture the entire tissue, and a region in the upper right can conduct only every other beat (Fig. 4B). When the tissue in this region cannot conduct, the isochrones crowd together and form a line of block.

In between the 1:1 and 2:1 regions, electrotonic effects (diffusive currents between cells) produce a region of 2:2 conduction, or alternans. It is important to note that this alternans does not arise as a direct consequence of rapid pacing,^{64,74,75} but strictly because of the interaction between the 1:1 and 2:1 regions. Fig. 5 shows optical action potentials from a series of sites spanning the 1:1 region proximal to the pacing site and 2:1 regions distal to the pacing site. Alternans of both APD and action potential amplitude (APA) develops in the transitional area between regions of 1:1 and 2:1 conduction. Action potential amplitude of alternating beats decreases in this region until block of alternating beats occurs.

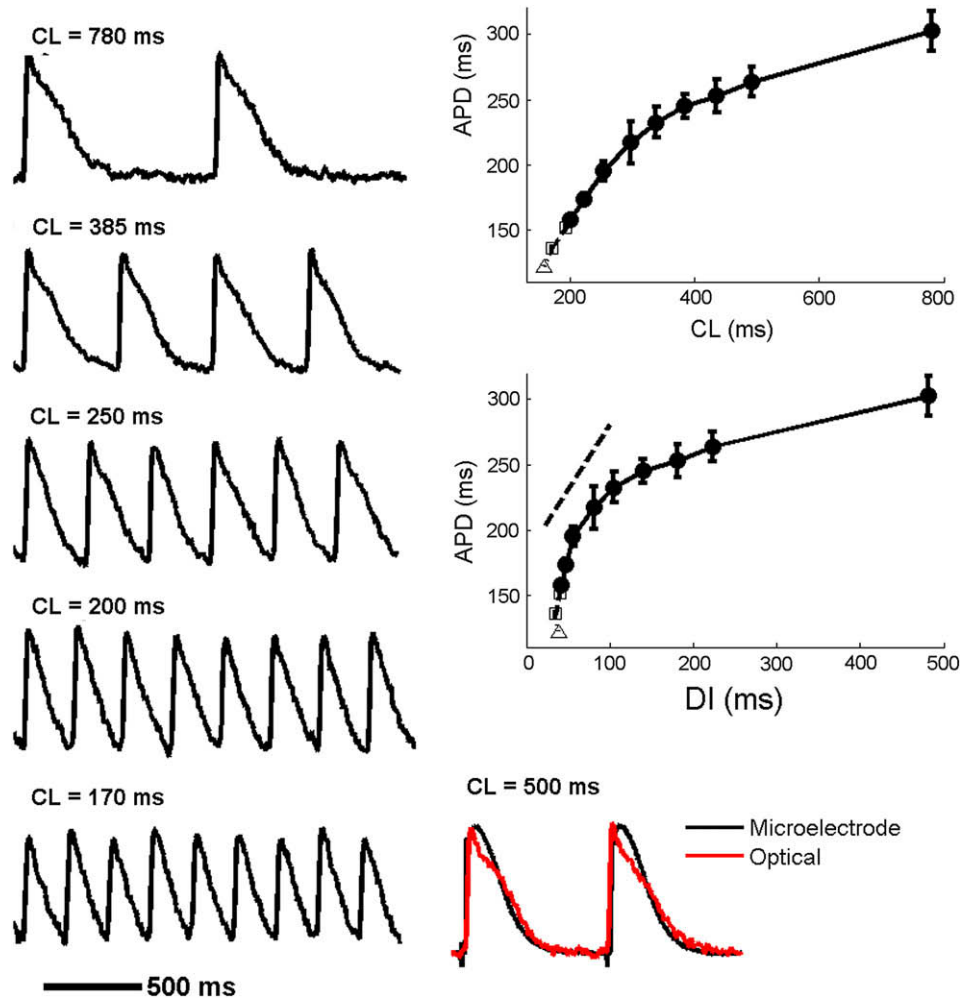


Figure 3 Optical action potentials and rate adaptation in equine atrial tissue. Representative action potentials obtained from one preparation using optical mapping are shown for a range of cycle lengths. Action potential durations (APDs) are shown as a function of cycle length (CL, top) and diastolic interval (DI, bottom). The dotted line in the APD vs. DI plot has slope one and indicates that the steepest portion of the restitution curve has slope greater than one. Data from four sites are averaged for the longer cycle lengths (circles/solid line), while data for the second- and third-smallest cycle lengths (squares/dashed line) were obtained from only three sites because of the occurrence of 2:1 block in the fourth site at these CLs. For the smallest cycle length (triangles), only one site did not exhibit 2:1 block. Error bars indicate maximum difference between the average value and the individual values obtained. APDs are computed as 90 percent of repolarization. Optical action potentials (red) are shown together with microelectrode action potentials (black) obtained from a different equine atrial preparation; both show similar triangular morphologies.

Induction of AF

The intrinsic dispersion of APD and DI can produce not only 2:1 conduction block, but also more complex Wenckebach patterns as the CL is decreased further. As the conduction patterns become more complex, propagation can fail in different directions at different times and initiate fibrillation. Fig. 6 shows how the spatial distribution of dominant frequencies changes with CL. Initially, only 1:1 propagation is present. Regions of 2:1 conduction arise by a CL of 500 ms, regions of 4:1 conduction occur by a CL of 250 ms, and

Wenckebach conduction appears between CLs of 220 and 170 ms. By the time a CL of 160 ms is reached, AF has initiated in the region of Wenckebach conduction. Because pacing is continued distal to this region, fibrillation is limited spatially and does not invade the rest of the tissue in this case.

Spatiotemporal dynamics of AF

Following cessation of rapid pacing (CL < 160 ms), fibrillation arises throughout the tissue. Fig. 7 shows two examples of AF initiated in different

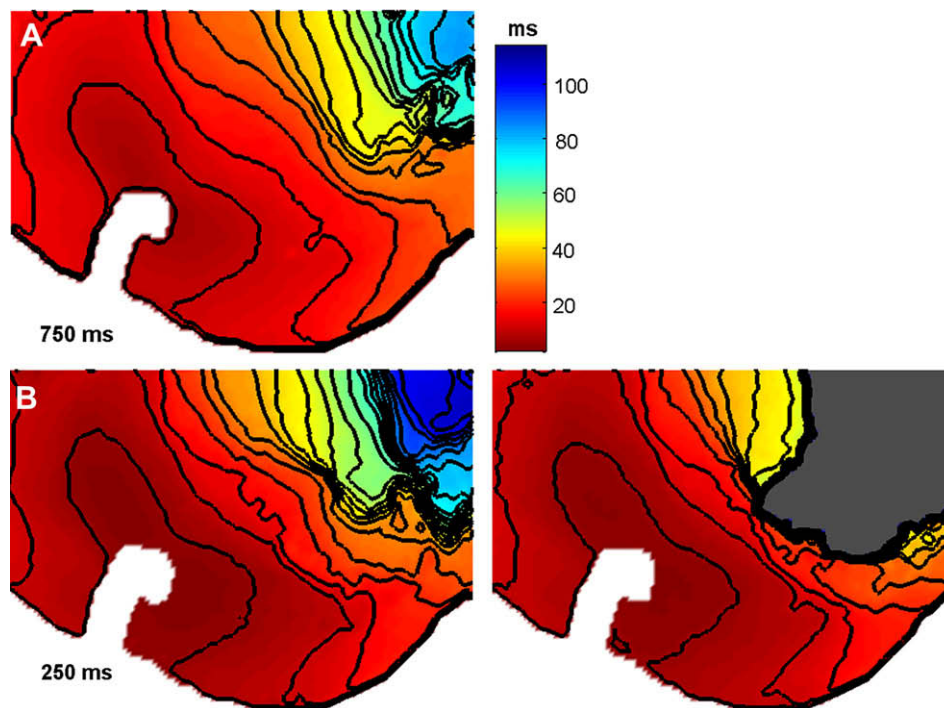


Figure 4 Activation isochrones at two different cycle lengths shown every 5 ms. (A) At a cycle length of 750 ms, the activation proceeds rapidly through the tissue from the pacing site (white area obscuring the tissue at lower left) but with slowing and crowding of isochrones in the upper right corner. (B) At a cycle length of 250 ms, not all of the tissue is activated on every beat, so two successive beats are shown, with gray indicating an area of block for the second beat. Conduction is slower relative to the longer cycle length, and there is more pronounced crowding of isochrones in the upper right corner. Activation times are measured at each site as the time at which depolarization has reached half of the full action potential amplitude.

preparations. Both examples show a wide variation in frequencies present, although both have large regions with lower frequencies together with smaller, higher-frequency areas. The electrical dynamics are complex with non-repeating patterns (also see movies in online [Supplement](#)).

Although fibrillation could be induced by rapid pacing, these arrhythmias were not sustained in all cases (<3 min). To induce sustained AF, it was necessary to add ACh (1–20 μM) to the perfusate. [Fig. 8](#) shows the spatiotemporal dynamics of AF induced using 1 μM ACh in two preparations. Higher concentrations of ACh resulted in higher frequencies (up to 15 Hz with the highest ACh concentrations), but the frequency distributions and electrical activations remained similar.

Effects of quinidine on AF

Non-sustained AF was inducible with rapid pacing in two of the preparations in the absence of ACh (Group I). In each of these preparations, sustained AF was inducible with 1 μM ACh. In one of these preparations (horse 1), sustained AF was terminated by 12 μM quinidine. Sustained AF could be

reinitiated in this preparation in the presence of 2 μM ACh, and this sustained AF was terminated by perfusion with 12 μM quinidine. Following perfusion with 12 μM quinidine in the presence of 2 μM ACh, only non-sustained AF could be reinitiated in this preparation. Sustained AF was terminated by 6 μM quinidine in the other Group I preparation (horse 2), and sustained AF could not be re-initiated in this preparation with either 1 or 2 μM ACh and rapid pacing.

Preparations in Group II required ACh perfusion to initiate AF. In one of these preparations (horse 3), 4 μM ACh induced non-sustained AF and 6 μM ACh initiated sustained AF. This sustained AF was terminated by perfusion with 1.2 μM quinidine, and sustained AF could not be reinitiated. In the other Group II preparation (horse 4), 8 μM ACh initiated sustained AF, which was terminated by perfusion with 6 μM quinidine. Non-sustained AF could not be reinitiated in this preparation after perfusion with either 8 μM or 10 μM ACh and 6 μM quinidine. Following perfusion of this preparation with 20 μM ACh, sustained AF was initiated by rapid pacing. Perfusion with 6 μM quinidine terminated AF and non-sustained AF could not be

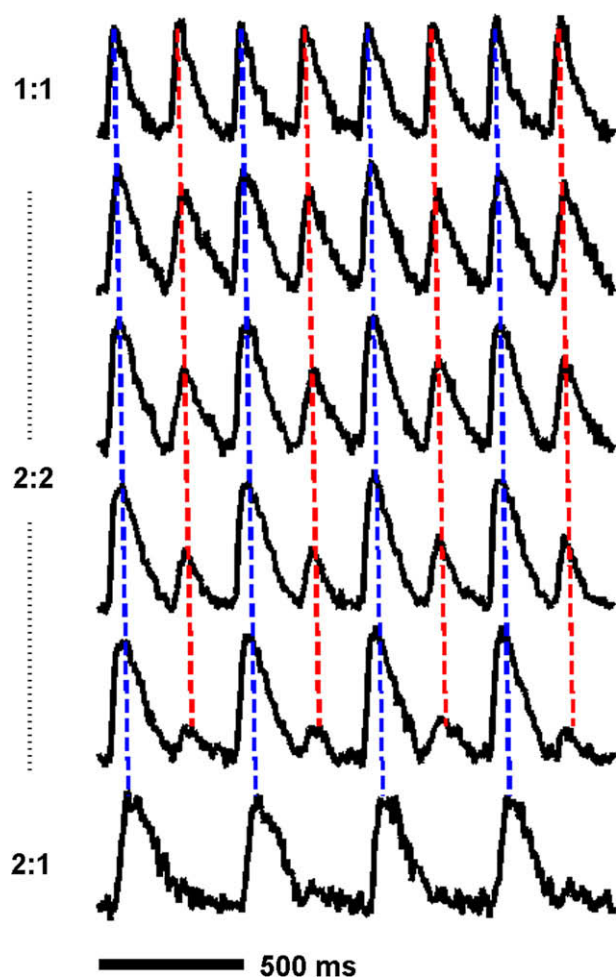


Figure 5 Development of alternans between regions of 1:1 and 2:1 conduction. Because some regions of the tissue have a larger minimum diastolic interval, regions that conduct every beat (1:1) may be present with regions that conduct only every other beat (2:1) at some cycle lengths. In between these regions, alternans (2:2) can arise because of electrotonic effects. In this case, successive action potentials vary in amplitude and duration. Here odd beats (blue) propagate throughout the tissue, but a marked reduction in action potential amplitude can be observed on even beats (red) as a wave propagates from a region of 1:1 conduction to a region of 2:1 conduction where block occurs.

reinitiated in this preparation under these conditions. These findings are summarized in Table 1.

Quinidine administration at concentrations between 1.2 and 12 μM terminated sustained AF in all trials in which sustained AF was inducible. Fig. 9 shows three examples of termination of sustained AF in different preparations with different quinidine dosages. In all trials in which quinidine terminated sustained AF, two phenomena were observed. The first was that the maximum dominant frequency decreased from 12–14 Hz (at high

ACh concentrations) or 7–11 Hz (at low ACh concentrations) gradually to 3–4 Hz immediately prior to AF termination, and the second was that the spatial distribution of frequencies became more homogenous, with larger regions of the tissue exhibiting the same dominant frequency.

Another important trend was that quinidine administration made the reinduction of fibrillation more difficult. Fig. 10 shows two examples of AF induced in the presence of quinidine that terminated within two seconds of induction. Note that the same two phenomena observed with termination of sustained AF by quinidine (Fig. 9) can be observed: Fig. 10A shows a reduction in the dominant frequency over large parts of the domain as the fibrillation begins to terminate, whereas Fig. 10B shows increased spatial homogeneity of the dominant frequency.

Discussion

Use of optical mapping to assess electrical activity

We present here the first study of electrical activity in equine cardiac preparations using optical mapping. The use of voltage-sensitive dyes to detect electrical activity in cardiac tissue is well established.^{16,45–64} The ANEP (Amino-Naphthyl(Ethenyl)Pyridium) group of dyes in particular has been used extensively to detect action potentials in excitable tissue due to its favorable signal-to-noise ratio and high fluorescence change with cellular depolarization.⁶⁹ The molecular structure of these compounds allows them to become anchored in the extracellular aspect of the membrane via two hydrophobic carbon chains of variable length, with the stability of this anchoring process being proportional to hydrocarbon chain length. Upon excitation of the dye by the appropriate wavelength (excitation frequency), the positive charge that rests in the pyridinium nitrogen is passed via resonance to the aniline nitrogen. This increases the dipole on the molecule, and when the cation moves back toward the anion sulphur moiety bound to the pyridinium nitrogen during the return to ground state, the absorbed energy is released as light (emission frequency).⁷⁶

Since the excitation frequency is higher than the emission frequency in these compounds, filters can be used to quantify relative changes in fluorescence. The amplitude of this “shift” in fluorescence upon excitation can be affected by the electric field that is induced by the passage of an

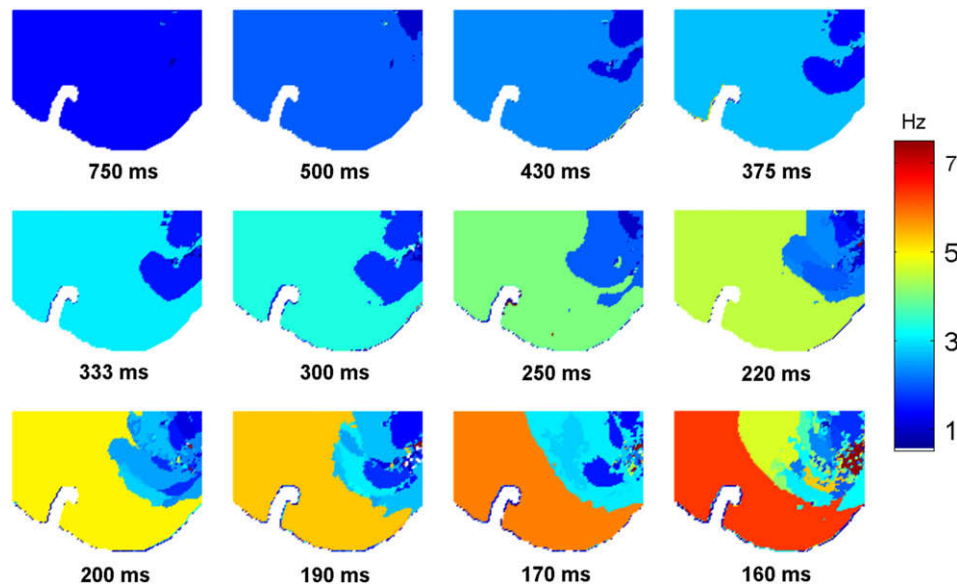


Figure 6 Spatial frequency distributions obtained for a range of CLs. As the CL is decreased, an area of 2:1 block develops distal to the pacing site (white area obscuring the tissue at lower left), in the upper right corner. The area of block grows as the CL is further decreased and more complex patterns of block develop, such as the presence of both 2:1 and 4:1 regions of block at a CL of 250 ms. At the shortest CLs, the frequency pattern becomes more complex with Wenckebach conduction. Dominant frequencies were determined during 6 s windows for each CL.

action potential along the membrane. The resulting signal is inversely proportional to the membrane potential and can be monitored with CCD cameras, and the output of this change can be used to track the propagation of electrical wave fronts in excitable tissue.

Restitution and alternans in equine atrial tissue

We have found that equine atrial preparations have steeply sloped restitution curves (maximum slope of 3.2). Although restitution curve slope

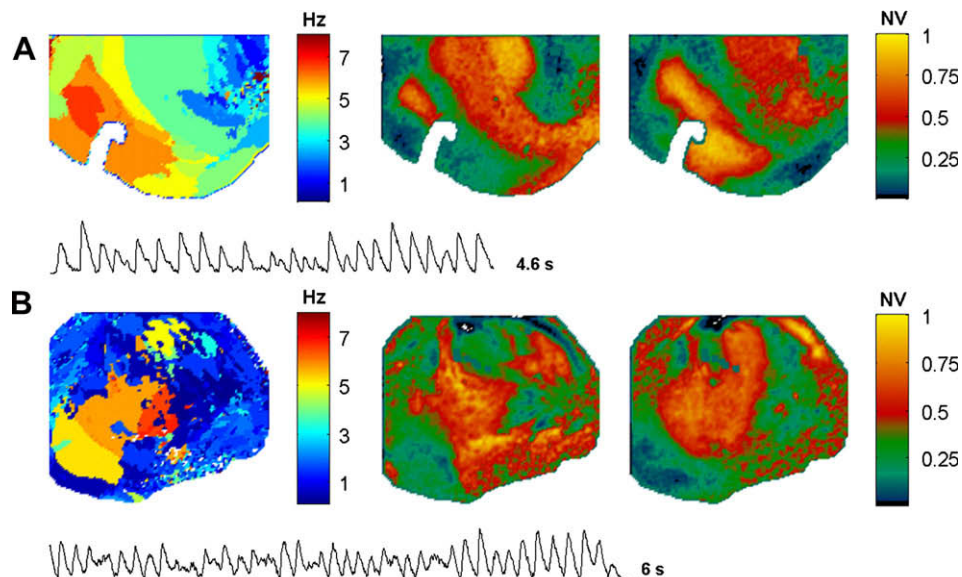


Figure 7 Spatiotemporal dynamics of non-sustained atrial fibrillation without acetylcholine perfusion in two preparations. Spatial frequency distribution, normalized voltage (NV) maps showing complex and changing patterns during the arrhythmia, and the optical signal from a single pixel are shown for each preparation. In both cases, AF self-terminated after less than one minute. Dominant frequencies were determined during (A) 4.4 s and (B) 4 s windows. NV maps are shown at times (A) 1.5 and 1.8 s and (B) 6.4 and 8.4 s. White area within the tissue region in (A) is tissue obscured by the pacing electrode.

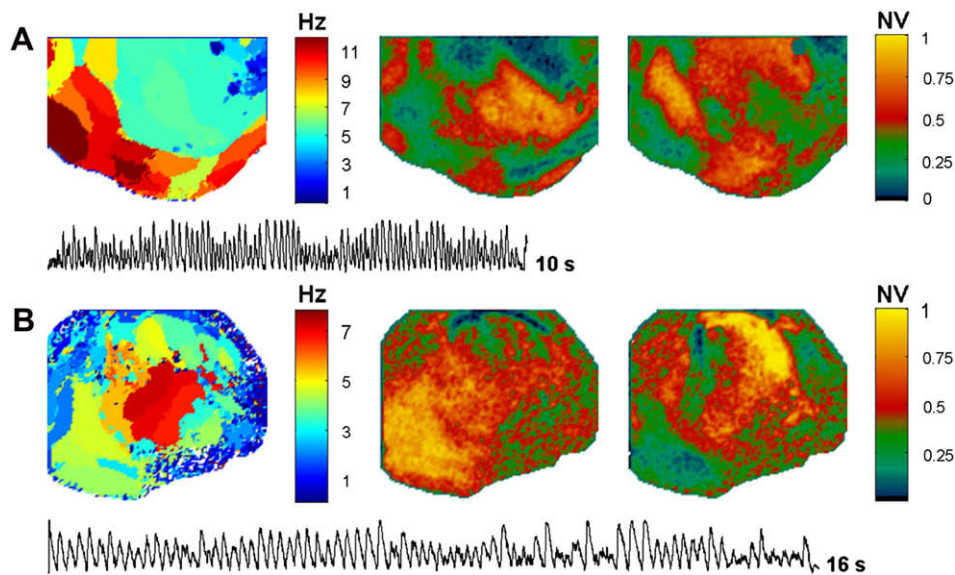


Figure 8 Spatiotemporal dynamics of sustained atrial fibrillation with acetylcholine perfusion in two preparations. Spatial frequency distribution, normalized voltage (NV) maps showing complex and changing patterns during the arrhythmia, and the optical signal from a single pixel are shown for each preparation. The concentration of ACh was $1 \mu\text{M}$ in both cases. Dominant frequencies were determined during 5 s windows. NV maps are shown at times (A) 1.8 and 3.2 s and (B) 15.4 and 15.5 s.

greater than one has been suggested as a predictor for alternans arising from rapid pacing,^{74,75} equine atrial tissue, like porcine ventricular tissue⁶³ and bullfrog myocardium,⁷⁵ shows no alternans at the pacing site despite steeply sloped restitution curves. Both electrotonic⁷⁷ and memory^{77,78} effects may be responsible for the absence of alternans.

In contrast, alternans was found to arise as a mediator between regions of 1:1 conduction and regions of 2:1 block. It is important to note that this type of alternans differs from alternans induced by

rapid pacing, where alternans originates at the pacing site (producing a region of 2:2) and conduction velocity can convert alternans from spatially concordant to spatially discordant,^{79–81} thereby providing nodes (regions of 1:1). In this scenario, large alternans amplitudes can lead to conduction block^{80–82} distal to the pacing site in a region beyond the first node. Here, alternans does not arise at the pacing site as 1:1 conduction is maintained. Block occurs distal to the pacing site, and spatially concordant alternans develops because of electrotonic effects. Each action

Table 1 Concentrations of acetylcholine (ACh) and quinidine (Quin) during induction and termination of non-sustained (NS) and sustained (S) arrhythmias in equine atrial preparations. For preparations with sustained fibrillation, concentrations of quinidine required to terminate fibrillation ($[\text{Quinidine}]_{\text{term}}$) and to prevent subsequent reinduction of sustained fibrillation ($[\text{Quinidine}]_{\text{prev,S}}$) or any fibrillation ($[\text{Quinidine}]_{\text{prev}}$) are indicated.

Group	Horse	Trial	[ACh] (mM)	$[\text{Quin}]_{\text{term}}$ (μM)	$[\text{Quin}]_{\text{prev,S}}$ (μM)	$[\text{Quin}]_{\text{prev}}$ (μM)
I	1	1	0 (NS)	n/a	n/a	n/a
		2	1 (S)	12	12	n/a
	2	1	0 (NS)	n/a	n/a	n/a
		2	1 (S)	6	6	6
		3	2	6	6	6
	II	3	1	1 (NS)	n/a	n/a
2			4 (S)	1.2	6	6
3			4 (S)	6	6	6
4		4	6 (S)	6	6	12
		1	8 (S)	6	6	6
		2	10 (S)	6	6	6
		3	20 (S)	6	6	6

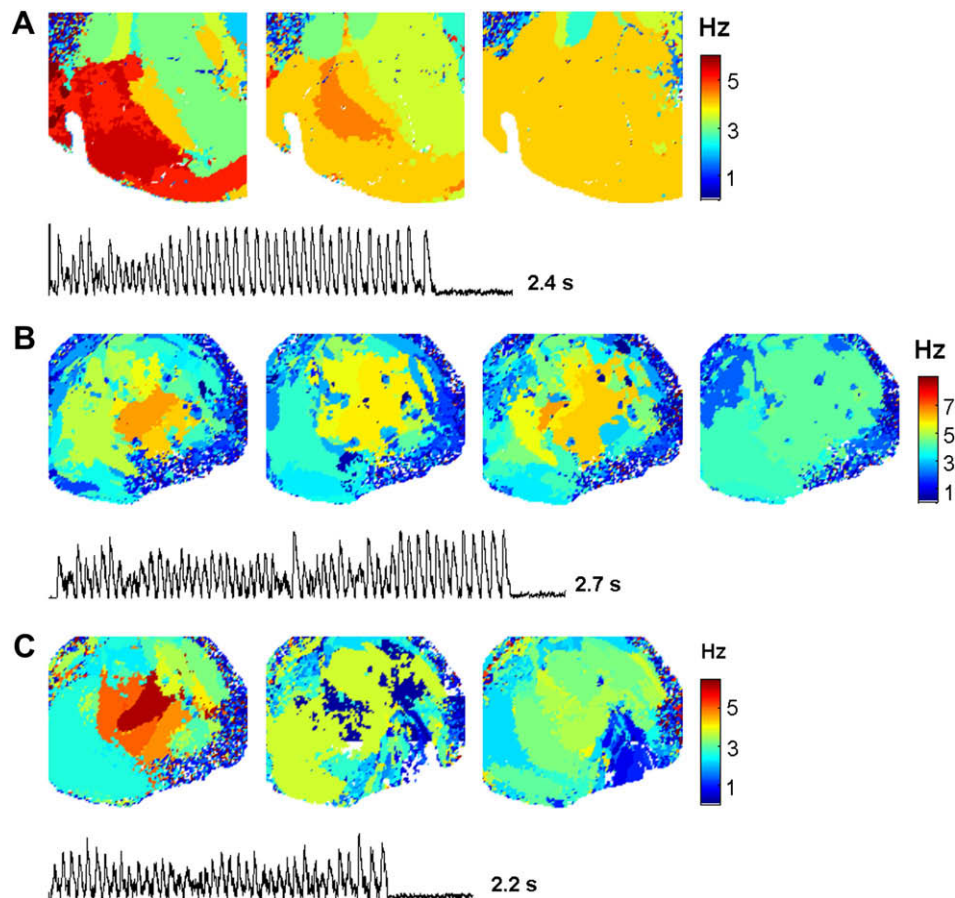


Figure 9 AF termination by quinidine. Spatial frequency distributions and the optical signal from a single pixel are shown. Maximum dominant frequencies decreased from 5–7 Hz to 3–4 Hz before arrhythmia termination. (A) Concentrations of ACh and quinidine were 2 and 12 μM , respectively. Dominant frequencies were determined during consecutive 2 s windows. White area at lower left is tissue obscured by the pacing electrode. (B) Concentrations of ACh and quinidine were 4 and 1.2 μM , respectively. Dominant frequencies were determined during 4 s windows, with the last three windows beginning 20, 32, and 50 s after the first window. (C) Concentrations of ACh and quinidine were 6 μM and 6 μM , respectively. Dominant frequencies were determined during consecutive windows, with the first window 3.4 s and the remaining two windows 4 s in duration.

potential that propagates from the 1:1 region but blocks in the 2:1 region undergoes a gradual decrease in amplitude, from full amplitude to zero amplitude within the region of block, thereby producing a 2:2 region. Although this mechanism for alternans development has been postulated theoretically to occur in the presence of ischemia,^{83–85} it has not been demonstrated previously in normal tissue or in an experimental setting.

Mechanisms of equine atrial fibrillation

Atrial fibrillation is a significant cause of morbidity and poor performance in horses, with an incidence of between 1 and 2% of the equine population evaluated by veterinarians annually.^{7,28,43} Most commonly diagnosed as a lone abnormality without associated gross cardiac structural

pathology, the mechanism of AF in horses previously has been the subject of research, both as an important veterinary clinical entity and as a naturally occurring model of human AF.^{86,88}

We have shown that equine AF arising from rapid pacing in vitro occurs in conjunction with the development of regions of conduction block and Wenckebach conduction. These patterns result from intrinsic or dynamic spatial variability in APD and DI. Variability in restitution curve properties, including maximal slope values and minimum DIs, has been shown to occur in human ventricles⁸⁷ and theoretical studies have indicated that such variability may give rise to reentry, independent of restitution curve slope values.^{87,88}

In this study, we have found that during AF there is no single dominant frequency for the entire preparation. Instead, multiple frequencies

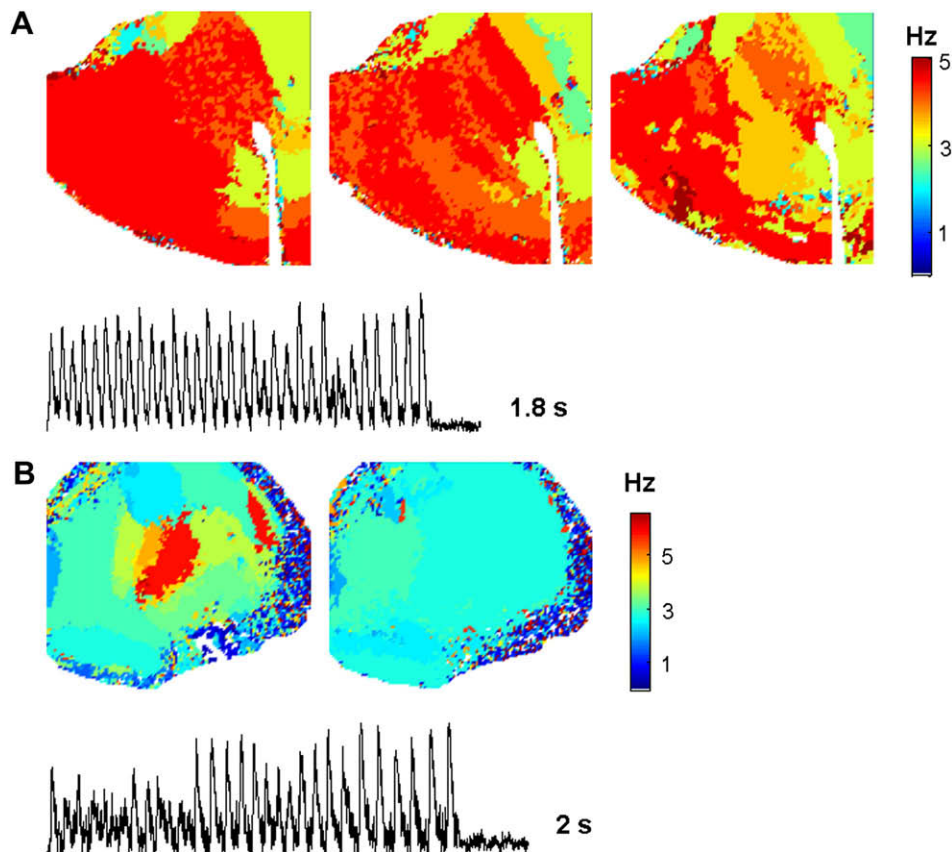


Figure 10 Self-termination of induced AF in the presence of quinidine. Spatial frequency distributions and the optical signal from a single pixel are shown. After initiation of AF, dominant frequency and spatial heterogeneity of frequencies decreased. (A) Concentrations of ACh and quinidine were 2 and 12 μM , respectively. Dominant frequencies were determined during consecutive 2 s windows. Because fibrillation terminates abruptly, the last spatial frequency map still includes frequencies present during fibrillation. White area at lower right in (A) is tissue obscured by the pacing electrode. (B) Concentrations of ACh and quinidine were 6 and 12 μM , respectively. Dominant frequencies were determined during consecutive 4 s windows.

are present simultaneously due to the presence of regions of conduction block. These frequencies ranged from 1 Hz to 8 Hz for AF induced by rapid pacing without ACh. Although the spatial distribution of frequencies may be interpreted as support for a single reentrant source located in the region with the highest dominant frequency, our optical mapping data show that multiple waves are present with non-repeating patterns. Reentrant waves rarely lasted for a full rotation. In this case, the presence of multiple frequencies arose because different regions of the tissue could be captured at different rates, and no single source could be identified in the region with the highest frequency, as shown in the movies in the [Supplement](#).

The range of maximal frequencies observed from rapid pacing-induced AF was similar to the dominant frequencies reported by Gelzer et al. using surface ECGs and intraatrial electrograms in

conscious horses with naturally occurring AF (5.76–8.51 Hz).⁸⁶ Although AF was not sustained when initiated without ACh, the range of frequencies observed with sustained AF induced with ACh was similar, although slightly higher than that observed with non-sustained AF in the absence of ACh, with frequencies as high as 15 Hz observed with higher ACh concentrations. Moreover, the spatial pattern of frequency domains was similar with and without ACh.

Quinidine as antiarrhythmic therapy for equine AF

Oral quinidine has been the cornerstone of antiarrhythmic therapy for equine AF for decades and is successful at converting horses with lone AF in approximately 85% of cases.^{7,28} Although the side effects of quinidine therapy in horses are not trivial, the relatively high efficacy of quinidine, its

availability, the lack of well characterized pharmacologic options, and cost and risk associated with electrical cardioversion have combined to establish quinidine as the standard of care for equine atrial fibrillation. In spite of its broad use in clinical veterinary medicine, the definitive mechanism of action of quinidine in the conversion of AF to NSR in horses has not been established.

Although it is known that Class I antiarrhythmics produce conduction slowing and refractory period prolongation, the mechanism by which they terminate AF has been the subject of debate for some time. Viewed in light of the multiple wavelet reentry hypothesis of Moe, AF is believed to be due to multiple reentrant waves that travel through the atrial myocardium.¹⁵ The size of each of these wavelets is determined by their wavelength, which can be defined as the product of the APD and conduction velocity (CV). In normal atrial myocardium, APD and CV promote a relatively long wavelength, leading to the development of a small number of relatively large, meandering reentrant waves that can collide and eventually self-terminate. Reduction of wavelength in diseased myocardium can promote the development of multiple smaller waves that all fit in the domain, resulting in sustained AF. This forms the basis for the hypothesis that an increase in wavelength promotes the development of larger reentrant waves that are more likely to terminate because they cannot fit. However, this may not be the mechanism by which quinidine terminates atrial arrhythmias. Quinidine is a Na⁺ channel blocker that decreases CV, but it has been shown to slightly increase APD while preferentially prolonging the effective refractory period (ERP) at short cycle lengths.³⁷ Therefore, the wavelength may remain relatively unaffected by quinidine administration. This apparent contradiction may be explained by the known increased ERP produced by quinidine.^{37,42}

Increased ERP may underlie the decrease in heterogeneity observed with quinidine perfusion, and suggests that the mechanism by which quinidine terminates equine AF may not involve alterations of wavelength, but rather an increase in minimum DI, allowing only lower frequencies throughout the tissue, and subsequent abolition of Wenckebach conduction. This hypothesis is supported by the finding that quinidine application resulted in a decrease in maximal dominant frequency. In our studies, the optical mapping frequency domains in all preparations mapped indicate that the termination of AF in the presence of quinidine is accompanied by a decrease in the maximal dominant frequency and by an increase in

the spatial homogeneity of the frequencies present (see Fig. 9). In all trials, termination occurred when the frequency reached 3–4 Hz. Gelzer et al. reported a similar decrease in the frequency upon quinidine administration, and termination also occurred when the arrhythmia frequency reached between 3 and 4 Hz in conscious horses with naturally occurring AF, suggesting that the source of the electrical impulses is slowed by quinidine in the intact horse.⁸⁶ One major limitation, however, was that the non-invasive nature of that study precluded determination of whether the dominant frequency in equine AF was the result of a single pacemaker focus, several synchronized spiral waves, or the activity of one reentrant wave. In addition, serum quinidine concentrations were not determined, which prevented a correlation from being made between drug concentration and electrophysiologic effects. Our studies suggest that equine AF can result from multiple reentrant waves within the atria of affected horses, and that the dominant frequency of AF decreases to 3–4 Hz immediately prior to AF termination at concentrations of quinidine that approximate those achieved in horses given clinically relevant doses of quinidine.

It is interesting to note that of the eight trials in which sustained AF was induced, termination of AF was achieved with concentrations of quinidine that are markedly lower than those that correspond to those that are considered therapeutic in the clinical setting in six of them (6 μ M in five trials, 1 μ M in one trial). Given this finding, it is tempting to speculate that termination of equine AF may be achieved in clinical cases with lower doses of quinidine or to question why conversion of AF has not been achieved with the administration of lower quinidine doses. A number of parameters, including the effects of the intact autonomic nervous system, stretch-activated receptors in the intact heart, and components of whole blood on the electrophysiology of atrial tissue and binding kinetics of quinidine may explain this discrepancy between our findings and the management of equine AF in clinical patients.

Limitations

One limitation of our study is that rate adaptation and restitution data were obtained only before administration of ACh and quinidine. For this reason, it was not possible to obtain quantitative information about the electrophysiological effects of either agent. Thus, a detailed mechanistic

explanation for the defibrillating effects of quinidine is beyond the scope of this work. Another limitation is that our work was by necessity performed *in vitro* and not *in vivo*. However, the similarities between the frequencies obtained here and those obtained *in vivo* by Gelzer et al.⁸⁶ suggest that the systems behave similarly. Another limitation of this study is that sharp electrode experiments designed to determine the effects of blebbistatin on action potential duration, amplitude, and morphology were, by necessity, performed on ventricular tissue. Given the scarcity of equine cardiac tissue, atria from all hearts harvested were reserved for optical mapping experiments. Previous studies, however, have shown that blebbistatin has minimal effects on these parameters in intact rabbit atrial and ventricular preparations and in cardiac myocytes isolated from rat ventricle.⁷¹ Given these findings, we are confident that blebbistatin is likely to have minimal effect on the electrophysiologic properties of equine atrial tissue. Finally, the number of preparations mapped was small, owing to the difficulty in procuring equine cardiac tissue suitable for mapping. For this reason, no detailed study of the effects of time on the viability of the preparation was performed. Nevertheless, optical signal quality and morphology did not appear to vary substantially over time.

Conclusions

Our study demonstrates, for the first time, that rapid pacing-induced AF in intact equine atrial preparations develops in conjunction with regions of conduction block and Wenckebach conduction resulting from spatial variability in the minimal DI for propagation. In addition, we found that AF is associated with multiple frequencies that are induced by regions of conduction block in intact equine atrial preparations, and that these frequencies correspond with those that have been documented in conscious horses with naturally occurring AF. We have also demonstrated for the first time experimentally the occurrence of a novel form of alternans that occurs as a result of electrotonic currents between regions with 1:1 and 2:1 conduction.

Our results also show that the termination of AF by quinidine in intact equine atrial preparations is associated with a decrease in the maximal dominant frequency and by an increase in spatial homogeneity of frequencies present, and that quinidine terminates AF in these preparations at concentrations that correspond to those achieved in horses given clinically relevant doses of

quinidine. In all cases in which quinidine terminated AF, termination was preceded by a slowing of dominant frequency. These findings are consistent with the hypothesis that the quinidine-induced increase in ERP results in an increase in minimum DI with subsequent abolition of Wenckebach conduction.

Acknowledgments

This work was supported in part by the National Institutes of Health under Grant no. HL075515-S03-S04 (F.H.F.) We thank Stefan Luther and Eberhard Bodenschatz for helpful suggestions and acknowledge their support from the Max Planck Society. We also thank Robert F. Gilmour, Jr. for helpful suggestions. We thank Patrick B. Burke and Michael W. Enyeart for expert technical assistance.

References

- Belloli C, Zizzadoro C. Atrial fibrillation in horses: difficult diagnosis for a therapeutic orphan. *Vet J* 2006;172:8–9.
- Deem DA, Fregin GF. Atrial fibrillation in horses: a review of 106 clinical cases, with consideration of prevalence, clinical signs, and prognosis. *J Am Vet Med Assoc* 1982;180:261–5.
- Young LE. Equine athletes, the equine athlete's heart and racing success. *Exp Physiol* 2003;88:659–63.
- De Clercq D, van Loon G, Baert K, Tavernier R, Croubels S, De Backer P, Deprez P. Effects of an adapted intravenous amiodarone treatment protocol in horses with atrial fibrillation. *Equine Vet J* 2007;39:344–9.
- Ohmura H, Hiraga A, Takahashi T, Kai M, Jones JH. Risk factors for atrial fibrillation during racing in slow-finishing horses. *J Am Vet Med Assoc* 2003;223:84–8.
- Stadler P, Deegen E, Kroker K. Echocardiography and therapy of atrial fibrillation in horses. *Dtsch Tierarztl Wochenschr* 1994;101:190–4.
- Reef VB, Levitan CW, Spencer PA. Factors affecting prognosis and conversion in equine atrial fibrillation. *J Vet Intern Med* 1988;2:1–6.
- van den Berg MP, Haaksma J, Brouwer J, Tieleman RG, Mulder G, Crijns HJ. Heart rate variability in patients with atrial fibrillation is related to vagal tone. *Circulation* 1997;96:1209–16.
- Coumel P. Paroxysmal atrial fibrillation: a disorder of autonomic tone? *Eur Heart J* 1994;15(Suppl. A):9–16.
- Brugada J. Electrophysiologic mechanisms of atrial fibrillation. *Rev Esp Cardiol* 1996;49(Suppl. 2):8–12.
- Abildskov JA. Additions to the wavelet hypothesis of cardiac fibrillation. *J Cardiovasc Electrophysiol* 1994;5:553–9.
- Cherry EM, Evans SJ. Properties of two human atrial cell models in tissue: restitution, memory, propagation, and reentry. *J Theor Biol*, doi:10.1016/j.jtbi.2008.06.030, in press.
- Moe GK. Evidence for reentry as a mechanism of cardiac arrhythmias. *Rev Physiol Biochem Pharmacol* 1975;72:55–81.
- Reumann M, Bohnert J, Osswald B, Hagl S, Doessel O. Multiple wavelets, rotors, and snakes in atrial fibrillation – a computer simulation study. *J Electrocardiol* 2007;40:328–34.
- Moe GK. On the multiple wavelet hypothesis of atrial fibrillation. *Arch Int Pharmacodyn Ther* 1962;140:183–8. 13.
- Berenfeld O, Zaitsev AV, Mironov SF, Pertsov AM, Jalife J. Frequency-dependent breakdown of wave propagation into

- fibrillatory conduction across the pectinate muscle network in the isolated sheep right atrium. *Circ Res* 2002;90:1173–80.
17. Cherry EM, Ehrlich JR, Nattel S, Fenton FH. Pulmonary vein reentry – properties and size matter: insights from a computational analysis. *Heart Rhythm* 2007;4:1553–62.
 18. Kalifa J, Tanaka K, Zaitsev AV, Warren M, Vaidyanathan R, Auerbach D, Pandit S, Vikstrom KL, Ploutz-Snyder R, Talkachou A, Atienza F, Guiraudon G, Jalife J, Berenfeld O. Mechanisms of wave fractionation at boundaries of high-frequency excitation in the posterior left atrium of the isolated sheep heart during atrial fibrillation. *Circulation* 2006;113:626–33.
 19. Kannel WB, Abbott RD, Savage DD, McNamara PM. Epidemiologic features of chronic atrial fibrillation: the Framingham study. *N Engl J Med* 1982;306:1018–22.
 20. Benjamin EJ, Wolf PA, D'Agostino RB, Silbershatz H, Kannel WB, Levy D. Impact of atrial fibrillation on the risk of death: the Framingham heart study. *Circulation* 1998;98:946–52.
 21. Wang TJ, Larson MG, Levy D, Vasan RS, Leip EP, Wolf PA, D'Agostino RB, Murabito JM, Kannel WB, Benjamin EJ. Temporal relations of atrial fibrillation and congestive heart failure and their joint influence on mortality: the Framingham heart study. *Circulation* 2003;107:2920–5.
 22. Wang TJ, Massaro JM, Levy D, Vasan RS, Wolf PA, D'Agostino RB, Larson MG, Kannel WB, Benjamin EJ. A risk score for predicting stroke or death in individuals with new-onset atrial fibrillation in the community: the Framingham heart study. *JAMA* 2003;290:1049–56.
 23. Rose RJ, Davis PE. The use of electrocardiography in the diagnosis of poor racing performance in the horse. *Aust Vet J* 1978;54:51–6.
 24. Buntenkotter S, Deegen E. Behaviour of the heart rate of horses with auricular fibrillation during exercise and after treatment. *Equine Vet J* 1976;8:26–9.
 28. Reef VB, Reimer JM, Spencer PA. Treatment of atrial fibrillation in horses: new perspectives. *J Vet Intern Med* 1995;9:57–67.
 29. Wang S, Morales MJ, Qu YJ, Bett GC, Strauss HC, Rasmusson RL. Kv1.4 channel block by quinidine: evidence for a drug-induced allosteric effect. *J Physiol* 2003;546(Pt 2):387–401.
 30. Clark RB, Sanchez-Chapula J, Salinas-Stefanon E, Duff HJ, Giles WR. Quinidine-induced open channel block of K⁺ current in rat ventricle. *Br J Pharmacol* 1995;115:335–43.
 31. Pugsley MK, Walker MJ, Saint DA. Block of NA⁺ and K⁺ currents in rat ventricular myocytes by quinacainol and quinidine. *Clin Exp Pharmacol Physiol* 2005;32:60–5.
 32. Snyders DJ, Hondeghem LM. Effects of quinidine on the sodium current of guinea pig ventricular myocytes. Evidence for a drug-associated rested state with altered kinetics. *Circ Res* 1990;66:565–79.
 33. Roden DM, Bennett PB, Snyders DJ, Balsler JR, Hondeghem LM. Quinidine delays IK activation in guinea pig ventricular myocytes. *Circ Res* 1988;62:1055–8.
 34. Bajaj AK, Kopelman HA, Wikswo Jr JP, Cassidy F, Woosley RL, Roden DM. Frequency- and orientation-dependent effects of mexiletine and quinidine on conduction in the intact dog heart. *Circulation* 1987;75:1065–73.
 35. Balsler JR, Bennett PB, Hondeghem LM, Roden DM. Suppression of time-dependent outward current in guinea pig ventricular myocytes. Actions of quinidine and amiodarone. *Circ Res* 1991;69:519–29.
 36. Johnson EA, Mc KM. The differential effect of quinidine and pyrilamine on the myocardial action potential at various rates of stimulation. *J Pharmacol Exp Ther* 1957;120:460–8.
 37. Franz MR, Costard A. Frequency-dependent effects of quinidine on the relationship between action potential duration and refractoriness in the canine heart in situ. *Circulation* 1988;77:1177–84.
 38. Packer DL, Grant AO, Strauss HC, Starmer CF. Characterization of concentration- and use-dependent effects of quinidine from conduction delay and declining conduction velocity in canine Purkinje fibers. *J Clin Invest* 1989;83:2109–19.
 39. Cha Y, Wales A, Wolf P, Shahrokni S, Sawhney N, Feld GK. Electrophysiologic effects of the new class III antiarrhythmic drug dofetilide compared to the class IA antiarrhythmic drug quinidine in experimental canine atrial flutter: role of dispersion of refractoriness in antiarrhythmic efficacy. *J Cardiovasc Electrophysiol* 1996;7:809–27.
 40. Brugada J, Sassine A, Escande D, Masse C, Puech P. Effects of quinidine on ventricular repolarization. *Eur Heart J* 1987;8:1340–5.
 41. Wu MH, Su MJ, Lue HC. Age-related quinidine effects on ionic currents of rabbit cardiac myocytes. *J Mol Cell Cardiol* 1994;26:1167–77.
 42. Rosenheck S, Sousa J, Calkins H, Kadish AH, Morady F. The effect of rate on prolongation of ventricular refractoriness by quinidine in humans.
 43. Morris DD, Fregin GF. Atrial fibrillation in horses: factors associated with response to quinidine sulfate in 77 clinical cases. *Cornell Vet* 1982;72:339–49.
 44. Muir 3rd WW, Reed SM, McGuirk SM. Treatment of atrial fibrillation in horses by intravenous administration of quinidine. *J Am Vet Med Assoc* 1990;197:1607–10.
 45. Dillon SM, Kerner TE, Hoffman J, Menz V, Li KS, Michele JJ. A system for in-vivo cardiac optical mapping. *IEEE Eng Med Biol Mag* 1998;17:95–108.
 46. Efimov IR, Nikolski VP, Salama G. Optical imaging of the heart. *Circ Res* 2004;95:21–33.
 47. Efimov IR, Huang DT, Rendt JM, Salama G. Optical mapping of repolarization and refractoriness from intact hearts. *Circulation* 1994;90:1469–80.
 48. Eloff BC, Lerner DL, Yamada KA, Schuessler RB, Saffitz JE, Rosenbaum DS. High resolution optical mapping reveals conduction slowing in connexin43 deficient mice. *Cardiovasc Res* 2001;51:681–90.
 49. Himel HD, Knisley SB. Comparison of optical and electrical mapping of fibrillation. *Physiol Meas* 2007;28:707–19.
 50. Liu YB, Peter A, Lamp ST, Weiss JN, Chen PS, Lin SF. Spatiotemporal correlation between phase singularities and wavebreaks during ventricular fibrillation. *J Cardiovasc Electrophysiol* 2003;14:1103–9.
 51. Mironov S, Jalife J, Tolkacheva EG. Role of conduction velocity restitution and short-term memory in the development of action potential duration alternans in isolated rabbit hearts. *Circulation* 2008;118:17–25.
 52. Ripplinger CM, Krinsky VI, Nikolski VP, Efimov IR. Mechanisms of unpinning and termination of ventricular tachycardia. *Am J Physiol Heart Circ Physiol* 2006;291:H184–92.
 53. Salama G, Choi BR. Imaging ventricular fibrillation. *J Electrocardiol* 2007;40(Suppl. 6):S56–61.
 54. Sakai T. Optical mapping of tachycardia-like excitation evoked by pacing in the isolated rat atrium. *Jpn J Physiol* 2004;54:593–9.
 55. Chen J, Mandapati R, Berenfeld O, Skanes AC, Gray RA, Jalife J. Dynamics of wavelets and their role in atrial fibrillation in the isolated sheep heart. *Cardiovasc Res* 2000;48:220–32.
 56. Hucker WJ, Fedorov VV, Foyil KV, Moazami N, Efimov IR. Images in cardiovascular medicine. Optical mapping of the human atrioventricular junction. *Circulation* 2008;117:1474–7.

57. Punske BB, Rossi S, Ershler P, Rasmussen I, Abel ED. Optical mapping of propagation changes induced by elevated extracellular potassium ion concentration in genetically altered mouse hearts. *J Electrocardiol* 2004;37(Suppl.):128–34.
58. Qu F, Ripplinger CM, Nikolski VP, Grimm C, Efimov IR. Three-dimensional panoramic imaging of cardiac arrhythmias in rabbit heart. *J Biomed Opt* 2007;12:044109.
59. Nanthakumar K, Jalife J, Massé Downar E, Pop M, Asta J, Ross H, Rao V, Mironov S, Sevaptsidis E, Rogers J, Wright G, Dhopeswarkar R. Optical mapping of Langendorff-perfused human hearts: establishing a model for the study of ventricular fibrillation in humans. *Am J Physiol Heart Circ Physiol* 2007;293:H875–80.
60. Rogers JM, Walcott GP, Gladden JD, Melnick SB, Kay MW. Panoramic optical mapping reveals continuous epicardial reentry during ventricular fibrillation in the isolated swine heart. *Biophys J* 2007;92:1090–5.
61. Banville I, Gray RA. Effect of action potential duration and conduction velocity restitution and their spatial dispersion on alternans and the stability of arrhythmias. *J Cardiovasc Electrophysiol* 2002;13:1141–9.
62. Bray MA, Lin SF, Wikswo J. Three-dimensional visualization of phase singularities on the isolated rabbit heart. *J Cardiovasc Electrophysiol* 2002;13:1311.
63. Banville I, Chattipakorn N, Gray RA. Restitution dynamics during pacing and arrhythmias in isolated pig hearts. *J Cardiovasc Electrophysiol* 2004;15:455–63.
64. Pastore JM, Girouard SD, Laurita KR, Akar FG, Rosenbaum DS. Mechanism linking T-wave alternans to the genesis of cardiac fibrillation. *Circulation* 1999;99:1385–94.
65. Girouard SD, Laurita KR, Rosenbaum DS. Unique properties of cardiac action potentials recorded with voltage-sensitive dyes. *J Cardiovasc Electrophysiol* 1996;7:1024–38.
66. Knisley SB, Justice RK, Kong W, Johnson PL. Ratiometry of transmembrane voltage-sensitive fluorescent dye emission in hearts. *Am J Physiol Heart Circ Physiol* 2000;279:H1421–33.
67. Nygren A, Clark RB, Belke DD, Kondo C, Giles WR, Witkowski FX. Voltage-sensitive dye mapping of activation and conduction in adult mouse hearts. *Ann Biomed Eng* 2000;28:958–67.
68. Sharifov OF, Fast VG. Optical mapping of transmural activation induced by electrical shocks in isolated left ventricular wall wedge preparations. *J Cardiovasc Electrophysiol* 2003;14:1215–22.
69. Salama G, Choi BR, Azour G, Lavasani M, Tumblev V, Salzberg BM, Patrick MJ, Ernst LA, Waggoner AS. Properties of new, long-wavelength, voltage-sensitive dyes in the heart. *J Membr Biol* 2005;208:125–40.
70. Finley MR, Li Y, Hua F, Lillich J, Mitchell KE, Ganta S, Gilmour Jr RF, Freeman LC. Expression and coassociation of ERG1, KCNQ1, and KCNE1 potassium channel proteins in horse heart. *Am J Physiol Heart Circ Physiol* 2002;283:H126–38.
71. Fedorov VV, Lozinsky IT, Sosunov EA, Anyukhovskiy EP, Rosen MR, Balke CW, Efimov IR. Application of blebbistatin as an excitation-contraction uncoupler for electrophysiological study of rat and rabbit hearts. *Heart Rhythm* 2007;4:619–26.
72. Cherry EM, Fenton FH. A tale of two dogs: analyzing two models of canine ventricular electrophysiology. *Am J Physiol Heart Circ Physiol* 2007;292:H43–55.
73. Bailey DN. Relative binding of therapeutic drugs by sera of seven mammalian species. *J Anal Toxicol* 1998;22:587–90.
74. Nolasco JB, Dahlen RW. A graphic method for the study of alternation in cardiac action potentials. *J Appl Physiol* 1968;25:191–6.
75. Guevara MR, Ward G, Shrier A, Glass L. Electrical alternans and period doubling bifurcations. *Comput Cardiol* 1984;11:167–70.
76. Loew L. Potentiometric dyes: imaging electrical activity of cell membranes. *Pure Appl Chem* 1996;68(7):1405–9.
77. Hall GM, Bahar S, Gauthier DJ. The prevalence of rate-dependent dynamics in cardiac tissue. *Phys Rev Lett* 1999;82:2995–8.
78. Cherry EM, Fenton FH. Suppression of alternans and conduction blocks despite steep APD restitution: electrotonic, memory, and conduction velocity effects. *Am J Physiol Heart Circ Physiol* 2004;286:H2332–41.
79. Tolkacheva EG, Schaeffer DG, Gauthier DJ, Krassowska W. Condition for alternans and stability of the 1:1 response pattern in a “memory” model of paced cardiac dynamics. *Phys Rev E* 2003;67:031904.
80. Watanabe MA, Fenton FH, Evans SJ, Hastings HM, Karma A. Mechanisms for discordant alternans. *J Cardiovasc Electrophysiol* 2001;12:196–206.
81. Qu Z, Garfinkel A, Chen PS, Weiss JN. Mechanisms of discordant alternans and induction of reentry in simulated cardiac tissue. *Circulation* 2000;102:1664–70.
82. Fenton FH, Cherry EM, Hastings HM, Evans SJ. Multiple mechanisms of spiral wave breakup in a model of cardiac electrical activity. *Chaos* 2002;12:852–92.
83. Choi BR, Jang W, Salama G. Spatially discordant voltage alternans cause wavebreaks in ventricular fibrillation. *Heart Rhythm* 2007;4:1057–68.
84. Bernus O, Zemlin CW, Zaritsky RM, Mironov SF, Pertsov AM. Alternating conduction in the ischaemic border zone as precursor of reentrant arrhythmias: a simulation study. *Europace* 2005;7(Suppl.):93–104.
85. Arce H, Lopez A, Guevara MR. Triggered alternans in an ionic model of ischemic cardiac ventricular muscle. *Chaos* 2002;12:807–18.
86. Gelzer AR, Moise NS, Vaidya D, Wagner KA, Jalife J. Temporal organization of atrial activity and irregular ventricular rhythm during spontaneous atrial fibrillation: an in vivo study in the horse. *J Cardiovasc Electrophysiol* 2000;11:773–84.
87. Nash MP, Bradley CP, Sutton PM, Clayton RH, Kallis P, Hayward MP, Paterson DJ, Taggart P. Whole heart action potential duration restitution properties in cardiac patients: a combined clinical and modeling study. *Exp Physiol* 2006;91:339–54.
88. Clayton RH, Taggart P. Regional differences in APD restitution can initiate wavebreak and re-entry in cardiac tissue: a computational study. *Biomed Eng Online* 2005;4:54.